Divergent activities of an engineered antibody in murine and human systems have implications for therapeutic antibodies

Carlos Vaccaro*, Roger Bawdon†, Sylvia Wanjie*, Raimund J. Ober*‡, and E. Sally Ward*§

*Center for Immunology, University of Texas Southwestern Medical Center, 6000 Harry Hines Boulevard, Dallas, TX 75390-9093; †Department of Obstetrics and Gynecology, University of Texas Southwestern Medical Center, 5323 Harry Hines Boulevard, Dallas, TX 75390-9032; and ‡Department of Electrical Engineering, University of Texas at Dallas, Richardson, TX 75083

Edited by Douglas T. Fearon, University of Cambridge, Cambridge, United Kingdom, and approved October 12, 2006 (received for review July 25, 2006)

The MHC class I-related receptor, neonatal Fc receptor (FcRn), plays a central role in regulating the transport and *in vivo* persistence of immunoglobulin G (IgG). IgG–FcRn interactions can be targeted for engineering to modulate the *in vivo* longevity and transport of an antibody, and this has implications for the successful application of therapeutic IgGs. Although mice are widely used to preclinically test antibodies, human and mouse FcRn have significant differences in binding specificity. Here we show that an engineered human IgG1 has disparate properties in murine and human systems. The mutant shows improved transport relative to wild-type human IgG1 in assays of human FcRn function but has short *in vivo* persistence and competitively inhibits FcRn activity in mice. These studies indicate potential limitations of using mice as preclinical models for the analysis of engineered antibodies. Alternative assays are proposed that serve as indicators of the properties of IgGs in humans.

antibody engineering | neonatal Fc receptor | half-life | human IgG1 | maternofetal transfer

Recent developments in antibody engineering have resulted in approaches that target the Fc region with the goal of altering effector functions such as Fcγ receptor-mediated cytotoxicity and *in vivo* persistence (1–6). As an IgG transporter, the neonatal Fc receptor (FcRn), serves to regulate the levels of IgG at diverse sites throughout the body by transporting IgGs within and across cellular barriers (7–13). The use of protein engineering, combined with knowledge of FcRn–IgG interactions at the molecular level, has resulted in approaches for the modulation of the persistence of antibodies *in vivo* (1, 3, 4, 14–17), which has direct relevance for the successful application of therapeutic antibodies.

Mice are routinely used as a readily accessible model for the preclinical evaluation of IgGs. Although human and mouse FcRn share sequence homology (18, 19), leading to the belief that mice might serve as reliable models for FcRn function across species, mouse FcRn unexpectedly has a much broader binding specificity relative to human FcRn (20, 21). In both humans and mice, FcRn–IgG interactions are characterized by pH-dependent binding with relatively high affinity at pH 6.0 that becomes progressively weaker as pH 7.2 is approached (15, 22–24). The model for FcRn-mediated transport is that IgG molecules are taken up by fluid phase pinocytosis and, subsequently, interact with this Fc receptor in acidic endosomes (25–27). Receptor-bound IgGs then are recycled or transcytosed and released at the cell surface by exocytic events that involve FcRn (28). This cellular transport mechanism is responsible for the homeostasis and transport of IgGs. As a result, for (engineered) IgGs, there is a strong correlation between the IgG-FcRn affinity (at pH ≈6.0), *in vivo* half-life, and transport across cellular barriers such as intestinal or lung epithelium and placental explants (1, 4, 13, 14, 17, 29, 30). However, this correlation breaks down if a significant increase in affinity is observed for binding of the IgG to FcRn at near-neutral pH (3, 31).

In the current study, we have generated an engineered human IgG1 antibody that has improved FcRn-mediated transport in human systems. The mutated variant has increased affinity for human FcRn and has been designed by targeting two residues (His-433 and Asn-434) in proximity to amino acids such as His-435 that play a central role in human FcRn–IgG interactions (2, 30, 32). However, these residues do not themselves make a major contribution to binding and therefore were chosen as targets for affinity improvement. Both human and mouse systems have been used to compare the functional activity of the mutant across species. Although analyses in human systems indicate increased transport of the mutant in human FcRn-mediated functions, testing in murine systems does not indicate this. The differences in behavior across species correlate with the distinct binding properties of the mutant IgG1 for mouse and human FcRn. The disparate activities of the mutated antibody in murine and human assays of FcRn function provide support for the concept that mice have limitations as models for the initial characterization of human IgGs. As an alternative, several human FcRn-based assays that are of utility in preclinical analyses are described.

Results

Binding of the Mutated IgGs to FcRn. During an analysis of the role of the nonconserved residue 436 (Tyr in humans and His in most murine isotypes; ref. 33) of human IgG1 in binding to human FcRn, we observed that mutation of this residue to histidine resulted in the loss of binding affinity (data not shown). This prompted us to generate a derivative of the triple HNY mutant (His-433 to Lys, Asn-434 to Phe, and Tyr-436 to His) described in ref. 3 in which only His-433 and Asn-434 were mutated to Lys-433 and Phe-434 (HN mutant) (Fig. 1*a*). Relative to the HNY mutant, the HN variant has an ≈2-fold higher affinity for binding to human FcRn at pH 6.0 (for HN, K_{D1} = 34 nM, Table 1; for HNY, K_{D1} = 82 nM). Importantly, the affinity for binding to the HN mutant is increased ≈16-fold over that for the wild-type human IgG1–human FcRn interaction (Table 1). In addition, the HN mutant binds with very low affinity to human FcRn at pH 7.2 that cannot be accurately determined under the conditions of the experiments (Fig. 1*b*). However, the binding of this mutant to human FcRn at pH 7.2 is slightly increased relative

Author contributions: E.S.W. designed research; C.V., R.B., S.W., and E.S.W. performed research; R.B. and R.J.O. contributed new reagents/analytic tools; C.V., S.W., R.J.O., and E.S.W. analyzed data; and R.J.O. and E.S.W. wrote the paper.

Conflict of interest statement: There is a pending patent that describes the mutated human IgG1 used in the studies.

This article is a PNAS direct submission.

Abbreviation: FcRn, neonatal Fc receptor.

§To whom correspondence should be addressed. E-mail: sally.ward@utsouthwestern.edu.

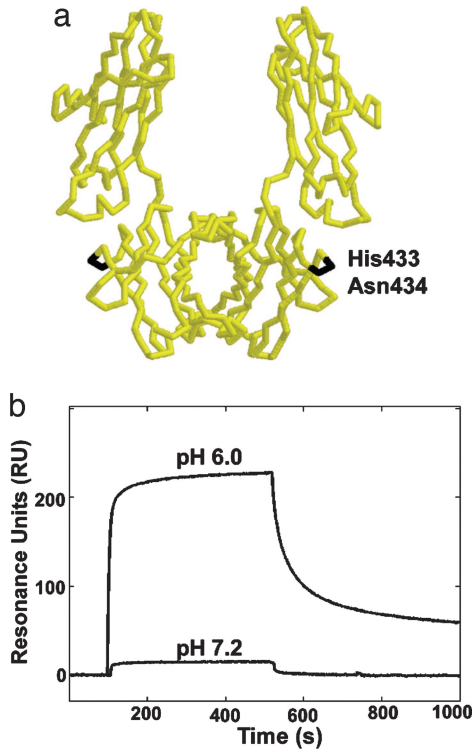

Fig. 1. The location of the mutations that constitute the HN mutant and binding of this mutant to human FcRn at pH 6.0 and 7.2. (*a*) α-carbon trace of human IgG1 (Fc region; ref. 48) with location of His-433 and Asn-434 shown. Figure was drawn by using Rasmol (courtesy of Roger Sayle, Bioinformatics Research Institute, University of Edinburgh, Edinburgh, U.K.). (*b*) Sensorgrams showing interaction of human FcRn with HN mutant at pH 6.0 and 7.2. Flow cells were coupled with HN mutant (622 RU) and recombinant human FcRn injected at a concentration of 250 nM in PBS plus 0.01% Tween 20, pH 6.0 or 7.2. All data are representative of duplicate injections and were zero adjusted, and reference cell data (flow cell coupled with buffer only during coupling cycle) was subtracted.

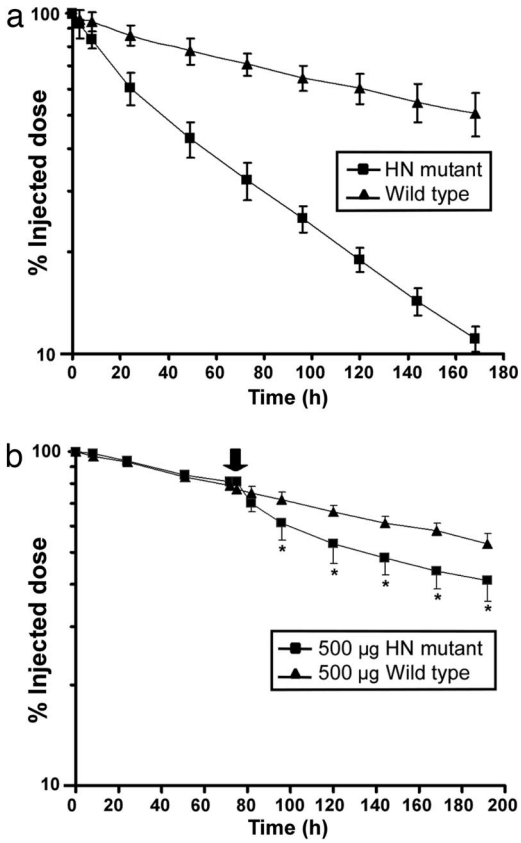

Fig. 2. The HN mutant has a relatively short half-life and enhances the clearance of ^{125}I-labeled wild-type human IgG1 in mice. (*a*) Swiss–Webster mice (five per group) were injected with ^{125}I-labeled IgGs, and radioactivity levels were assessed by whole-body counting. Data shown are mean values for each group, and bars indicate standard deviations. (*b*) Swiss–Webster mice (five per group) were injected with ^{125}I-labeled wild-type human IgG1, and 72 h later (indicated by arrow), were injected with 500 μg of wild-type human IgG1 or 500 μg of HN mutant. Levels of radioactivity in the mice were determined at the indicated times by whole-body counting. The data shown are means of remaining radioactivity in each group of mice. Error bars indicate standard deviations. *, data for these time points are significantly different, with $P < 0.02$ (Student's *t* test). Data are representative of two independent experiments.

to that of wild-type human IgG1 (Fig. 1*b*; refs. 3 and 31). In contrast, analyses of the interaction of mouse FcRn with the HN mutant indicate that, relative to human FcRn, this mutant has considerably increased binding affinities at both pH 6.0 and pH 7.2 (Table 1).

Properties of the HN Mutant in Mice. Initially, we analyzed the half-life of the HN mutant in mice. Consistent with earlier studies in mice in which IgG mutants with reduced pH dependence for FcRn binding were assessed (3), this mutant has short *in vivo* persistence relative to wild-type human IgG1, with a β-phase half-life of 62.8 $\pm$ 2.7 h (HN) that is significantly shorter than that of wild-type (250.6 $\pm$ 15.3 h) (Fig. 2*a*). The short *in vivo* half-life, together with the high affinity and reduced pH dependence of the HN mutant for binding to mouse FcRn, suggested that it might competitively inhibit FcRn activity i.e., act as an "Abdeg" (31) ("antibody that enhances IgG degradation"). This was investigated by analyzing the effect of this mutant on the clearance of radiolabeled wild-type human IgG1 from mice (Fig. 2*b*). Mice were injected with ^{125}I-labeled wild-type human IgG1 and 72 h later injected with 500 μg of HN mutant or, as a control, 500 μg of wild-type human IgG1. Levels of radioactivity in the mice were determined at the indicated times by whole body counting. The HN mutant induces a decrease in levels of ^{125}I-labeled IgG1 that is not seen in the control group of mice, with the levels of radioactivity decreasing to 41 $\pm$ 5% of the injected dose at 120 h after injection of the mutant.

Table 1. Equilibrium dissociation constants for interactions of wild-type IgG1 and HN mutant with mouse and human FcRn

FcRn species (pH)	Wild-type IgG1 K_{D1}, nM	HN mutant K_{D1}, nM
Human FcRn (6.0)	528	34
Human FcRn (7.2)	ND*†	ND*
Mouse FcRn (6.0)	32	1.5
Mouse FcRn (7.2)	ND*‡	82

*ND, not determined, because affinity was too low to accurately estimate under the conditions of the surface plasmon resonance experiments.
†Described in refs. 3 and 31.
‡Described in ref. 3.

Different Properties of the HN Mutant in Human and Mouse FcRn Expressing Cells. The disparate binding properties of the HN mutant for mouse and human FcRn, particularly the difference in pH dependence, suggested that the behavior in mouse models described above might not be predictive of that in human systems. We therefore compared the behavior of the HN mutant by using an *in vitro* assay in which the uptake and recycling of

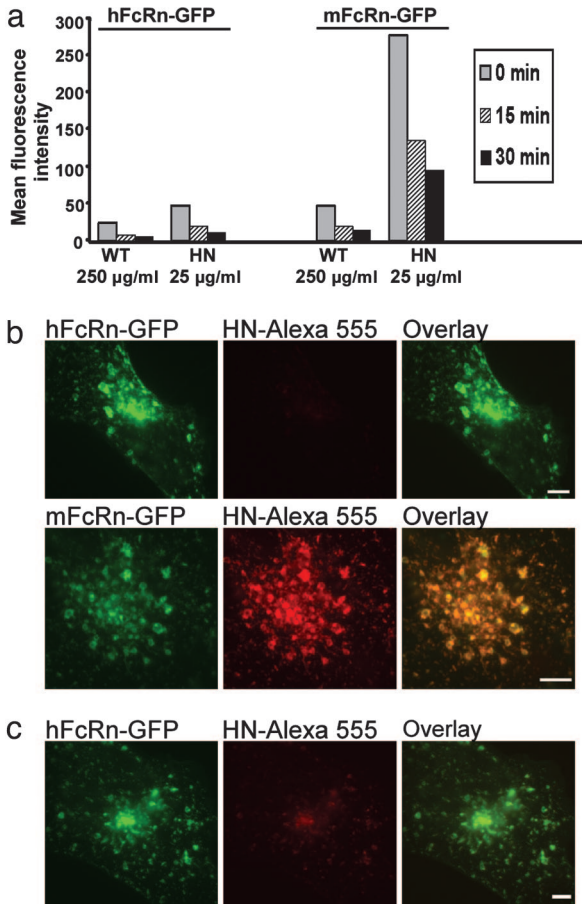

Fig. 3. The HN mutant shows different recycling behavior in human microvascular endothelial cell 1 cells transfected with human-GFP (hFcRn-GFP) or mouse FcRn-GFP (mFcRn-GFP). (*a*) Cells were pulsed with Alexa 647-labeled wild-type (WT) human IgG1 or HN mutant and then chased for 0, 15, or 30 min. Cell-associated fluorescence (Alexa 647) levels in GFP^+ cells were quantitated by flow cytometry and are expressed as mean fluorescence intensities. (*b*) Transfected cells were pulsed with Alexa 555-labeled HN mutant, washed, fixed, and imaged by fluorescence microscopy. Alexa 555-labeled HN mutant was imaged at the same exposure times for both mouse and human FcRn-GFP transfected cells. (*c*) As in *b*, except that a longer exposure time was used for imaging Alexa 555-labeled HN mutant. GFP and Alexa 555 are shown in green and red, respectively. (Scale bars: 5 μm.) Data shown are representative of at least two independent experiments.

labeled IgG by human or mouse FcRn-transfected endothelial cells was assessed. Human microvascular endothelial cell 1 cells were transfected with expression constructs encoding either human FcRn-GFP plus human β2-microglobulin or mouse FcRn-GFP plus mouse β2-microglobulin (27, 31). β2-microglobulin constructs were cotransfected to ensure that this protein was not limiting for functional expression (34, 35). Cells were incubated with HN mutant or wild-type human IgG1 (both labeled with Alexa 647), washed, and then chased in medium for different time periods. The amount of cell-associated fluorescence was determined by flow cytometry (Fig. 3*a*). In these experiments, Alexa 647 labeled wild-type human IgG1 was used at a 10-fold higher concentration ($\approx$1.6 μM; 250 μg/ml) relative to Alexa 647-labeled HN mutant, because this was necessary to detect significant levels of uptake, which for wild-type IgG1 is believed to occur primarily by fluid phase due to the pH dependence of the FcRn–human IgG1 interaction (3). In contrast, the altered binding properties of the HN mutant resulted in measurable uptake by both types of transfectants at a concentration of 25 μg/ml ($\approx$160 nM). Untransfected cells did not accumulate either antibody to detectable levels (data not shown), suggesting that the endogenous expression level of FcRn is low in these cells (in contrast to the human lung-derived endothelial cell line, HULEC-5A; ref. 36 and data not shown).

The data shown in Fig. 3*a* indicate that for human FcRn-transfected cells, both wild-type human IgG1 and HN mutant are recycled efficiently during a 30-min chase period, although the uptake of HN is initially higher than that of wild-type human IgG1 (Fig. 3*a* and data not shown). In contrast, the HN mutant accumulates to substantially higher levels relative to wild-type human IgG1 in mouse FcRn-transfected cells and, consistent with the marked loss of pH dependence of the mouse FcRn–HN mutant interaction, this IgG is not efficiently recycled out of the cells relative to wild-type human IgG1 (Fig. 3*a*). Further, the recycling behavior of the HN mutant in human FcRn transfectants bears some resemblance to that of wild-type human IgG1 in mouse FcRn transfectants (Fig. 3*a*).

Fluorescence microscopy analyses of IgG-pulsed cells were consistent with these differences in uptake and retention. Using similar exposure times, greater uptake of the HN mutant could be detected for cells transfected with mouse FcRn relative to human FcRn (Fig. 3*b*). For the latter, longer exposure times were needed to detect labeled IgG within cells (Fig. 3*c*). The data in Fig. 3 *b* and *c* demonstrate that the IgG colocalizes with FcRn in endosomes that are positive for early endosomal antigen-1 (ref. 27 and data not shown). Taken together, in mouse FcRn-transfected cells, the HN mutant has properties that are consistent with its ability to competitively inhibit FcRn function in mice (Fig. 2*b*). However, in human FcRn-transfected cells, this mutant has distinct characteristics that indicate improved FcRn-mediated transport.

Improved Transport of the HN Mutant Across the *ex Vivo* Placenta. The binding properties of the HN mutant for human FcRn, together with its behavior in transfected cells, suggested that it might be transported across the human placenta more efficiently than wild-type human IgG1. We have shown that this assay is a reliable indicator of human FcRn-mediated transport (30), which for ethical reasons cannot be assessed by pharmacokinetic analyses. We therefore compared the transport of the HN mutant with that of wild-type human IgG1 (Fig. 4). Assays were carried out with radioiodinated HN mutant plus biotinylated human IgG1 (Fig. 4*a*) and biotinylated HN mutant plus radioiodinated wild-type human IgG1 (Fig. 4*b*). From a total of three placental transfer experiments, transfer rates for the HN mutant were 0.091 $\pm$ 0.017% of maternal IgG per hour, whereas for wild-type human IgG1, they were 0.051 $\pm$ 0.020% of maternal IgG per hour. Collectively, the data demonstrate that the HN mutant is transported more efficiently from the maternal to fetal compartment.

Discussion

Recent interest in antibody engineering has expanded to the modulation of Fc function by targeting residues that interact with FcRs. One such FcR is FcRn that serves to regulate IgG transport and levels (37–40). Engineering FcRn–IgG interactions can lead to alterations in *in vivo* persistence and transfer across cellular barriers (1, 4, 13, 14, 17, 29, 30), which has implications for the optimal delivery of therapeutic IgGs (6). The purpose of this study was to evaluate the activity of an engineered human IgG1 in both human and murine systems. The engineering was designed to increase the activity of the IgG in human FcRn-mediated functions. As such, the antibody has mutations in the CH3 domain (His-433 to Lys and Asn-434 to Phe) that result in increased affinity at pH 6.0 with retention of pH dependence (i.e., very low affinity at near-neutral pH) for binding to human FcRn. Analyses in the placental transport

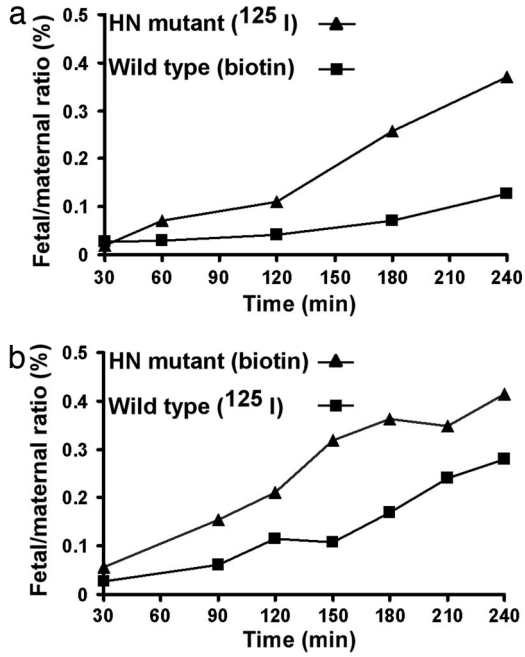

Fig. 4. The HN mutant is transported more efficiently relative to wild-type human IgG1 across the *ex vivo* placenta. Biotinylated and iodinated IgGs were premixed and added to the maternal compartment. Transport of each IgG into the fetal compartment was assessed from 30 min to 240 min after the addition. Data from two experiments in which the IgGs were differently labeled are shown.

model (30) and a human-based *in vitro* cell assay demonstrate that the mutated antibody behaves as designed. Specifically, relative to the wild-type antibody, transport across the placenta is improved and the *in vitro* cell assay shows increased recycling. In contrast, analyses in mice demonstrate that the HN mutant exhibits behavior that is distinct to that observed in human systems. This mutated IgG1 is not recycled efficiently by transfected cells expressing mouse FcRn and, importantly, has a decreased half-life in mice.

Our observations highlight the potential limitations of using murine systems as preclinical models for the assessment of therapeutic IgGs, for which the pharmacokinetics and distribution are key determinants of efficacy and assessment of side effects. The short *in vivo* persistence of a mutated human IgG, such as the HN mutant, in mice could lead to the conclusion that the mutant might not have the desired activity in humans. More importantly, the rapid clearance in mice might impact the therapeutic efficacy and side effects of the engineered antibody in a murine disease model. Given the differences in FcRn across species (20, 21), this discrepancy is not specific to only the HN mutant, but is expected to be general for both wild-type and mutated human IgGs. Collectively, our results point to a need for careful evaluation of preclinical data generated in mice, because relatively small differences in persistence and distribution can have far reaching functional consequences.

Discrepant behavior due to cross-species differences in FcRn might not occur only when (human) IgGs are mutated in regions proximal to the FcRn–IgG interaction site. Considerable interest in antibody engineering recently has focused on Fc engineering (including the alteration of glycosylation patterns) with the goal of modulating Fcγ receptor binding (2, 5, 6, 41, 42). However, alteration of amino acids that are distal to FcRn–IgG interaction sites or variations in glycosylation patterns may impact FcRn binding (2) and *in vivo* persistence (32, 43), which might have different manifestations across species.

Despite the differences in FcRn across species, mouse models have significant utility for the analyses of IgGs that have similar binding properties for both mouse and human FcRn and also in the analyses of principles for generating engineered antibodies. For example, if the affinities at both pH 6.0 and 7.2 of an engineered IgG for mouse FcRn are well characterized, then this can be correlated with *in vivo* data to determine whether these properties confer increased serum half-life or, at the other extreme, the ability to inhibit FcRn function and act as an Abdeg (31). Specifically, the fundamental mechanistic principles of antibody behavior in mice and humans are predicted to be shared across species. As a consequence, initial studies in mice can give valuable correlative data between interaction characteristics and activity that is of relevance to FcRn function in humans.

In the current study, the marked differences in properties of the HN mutant in murine and human systems can be explained by the observation that the affinity increases at both pH 6.0 and near-neutral pH are much greater for mouse FcRn relative to the affinity improvements for the human receptor. Similarly, in an earlier study, increased affinities combined with the loss of pH dependence of human IgG1-derived mutants for binding to mouse FcRn resulted in short *in vivo* persistence (3). Consistent with the binding properties of the HN mutant for mouse FcRn, this IgG inhibits FcRn function and enhances the clearance of wild-type human IgG1 in mice. The HN mutant therefore has activity as an Abdeg (31).

However, the activity of the HN mutant as an Abdeg is not as potent as that of the MST-HN mutant that we described in ref. 31. The MST-HN mutant is a derivative of human IgG1 that comprises the HN mutations in addition to mutations of Met-252, Ser-254, and Thr-256 to Tyr-252, Thr-254, and Glu-256, respectively. The most likely reason for the lower activity is that although the affinities of the HN and MST-HN mutants for mouse FcRn are similar at pH 6.0, the affinity of the HN mutant at pH 7.2 is $\approx$10-fold lower (82 nM for HN vs. 7.4 nM for MST-HN; Table 1 and ref. 31, respectively). Similarly, relative to the HN mutant that binds to human FcRn at pH 7.2 with a low affinity that cannot be accurately determined (Fig. 1), the MST-HN mutant has substantially higher binding affinity for human FcRn at this pH (ref. 31 and K_{D1} = 224 nM; S.W. and E.S.W., unpublished data). This reduced pH dependence indicates that the MST-HN mutant will have Abdeg activity, rather than increased persistence, in humans. Analyses of the uptake and recycling of this mutant in human FcRn transfected endothelial cells support this prediction (C.V. and E.S.W., unpublished observations).

Although the loss of pH dependence is more marked for the interaction of the HN mutant with mouse FcRn, relative to wild-type human IgG1, there is also a small increase in binding of this mutant to human FcRn at pH 7.2 (Fig. 1; refs. 3 and 31). Nevertheless, the properties of this mutant endow improved transport across the placental barrier and in human FcRn-transfected endothelial cells. This indicates that the slightly reduced pH dependence does not impede release of IgG cargo during exocytic events (28). Importantly, our data in this study and in ref. 3 suggest that there may be a ceiling to the increase in affinity for FcRn–IgG interactions at pH 6.0 that is achievable if weak binding at pH 7.2 is to be retained, because, in general, affinity increases at pH 6.0 would be expected to be accompanied by increases at pH 7.2. As a consequence, one of the challenges in the engineering of IgGs for increased persistence is to substantially increase the affinity at pH 6.0 whilst retaining low enough affinity at near-neutral pH so that the IgG is efficiently recycled or transcytosed.

Significantly, our assays using mouse or human FcRn-transfected endothelial cells give functional readout of the disparate *in vitro* activities of the HN mutant in the two species: in mouse FcRn transfectants, the mutant accumulates to high

levels and is inefficiently recycled, whereas in human FcRn transfectants, lower accumulation is accompanied by more efficient recycling. Relative to wild-type human IgG1, the greater accumulation of the HN mutant in mouse FcRn-transfected cells is due to several reasons. First, its retention of good binding affinity at pH 7.2 ($K_D \approx 80$ nM) would be expected to enhance receptor-mediated uptake. Second, the loss of pH-dependence results in inefficient recycling due to poor release at the cell membrane during exocytic events (28).

Given the differences in binding specificity for FcRn between mice and humans (3, 21), our studies raise the question as to which readily accessible models are suitable for the early preclinical screening of IgGs before analyses in nonhuman primates? We show here that the transport of an IgG across the human placenta, combined with binding analyses and *in vitro* cell-based assays, are reliable indicators of human FcRn function (30). In this context, although mice that transgenically express human FcRn have been developed (40), these mice have abnormally low serum IgG levels due to the very poor binding of endogenous mouse IgGs to human FcRn (20). These mice crossed onto transgenic mice expressing human IgGs might circumvent this possible limitation and provide a useful model.

Taken together, our data indicate that the use of mice to assess the activity of engineered IgGs in FcRn-mediated functions needs to be combined with a thorough understanding of the biophysical nature of the relevant FcRn–IgG interactions. Specifically, analyses in mice of the pharmacokinetics and distribution of IgGs cannot be readily extrapolated to humans unless the IgG being studied has similar interaction properties for FcRn across species. However, given the generally higher affinity of IgGs for mouse FcRn relative to human FcRn (3, 21), similar characteristics across species are expected to be uncommon. In the current study, we have described assay systems that should be of utility in predicting the behavior of engineered IgGs in FcRn-mediated functions in humans.

Materials and Methods

Mice. Swiss–Webster mice (females, 6–8 weeks old) were purchased from Harlan Sprague (Indianapolis, IN). All mouse experiments were carried out with the approval of the Institutional Animal Care and Use Committee at the University of Texas Southwestern Medical Center.

Expression Plasmids. The expression plasmid for a humanized anti-lysozyme heavy chain (human IgG1) has been described in ref. 44 and was a generous gift of Jefferson Foote (Arrowsmith Technologies, Seattle, WA). Splicing by overlap extension with mutagenic oligonucleotides was used to generate the double mutant, His-433 to Lys and Asn-434 to Phe (HN mutant) and triple mutant, His-433 to Lys, Asn-434 to Phe, and Tyr-436 to His (HNY mutant). Sequences of oligonucleotides are available upon request. The mutations were made on an XmaI subfragment of the human IgG1 constant region gene by using XmaI sites in the CH3 domain (overlapping codons 14–16) and 3′ to the coding sequence. Standard methods were used to reconstruct the final expression constructs, and insertion of the desired mutations were verified by DNA sequencing.

Expression vectors for the production of human FcRn-GFP, mouse FcRn-GFP, and human and mouse β2-microglobulin have been described in refs. 27 and 31.

Recombinant Antibody Production. Transfectants expressing an anti-lysozyme-specific antibody containing the HN mutant were generated as described in refs. 30 and 44. Wild-type and mutated antibodies were purified from culture supernatants by using lysozyme-Sepharose (44).

Surface Plasmon Resonance Analyses. The interactions of wild-type and mutated human IgGs with recombinant human and mouse FcRn were analyzed by using methods as in Zhou *et al.* (21, 45). Equilibrium binding studies were carried out by using PBS, pH 6.0 or 7.2 plus 0.01% (vol/vol) Tween 20 and 0.02% wt/vol sodium azide as running buffer. Experiments were carried out by using programmed methods and repeat injections to ensure that there was no significant loss of ligand-binding activity during the course of the experiment (46). After the dissociation phase for each injection (200–2,000 seconds), flow cells were stripped with PBS, pH 7.2/0.01% Tween 20/0.02% wt/vol sodium azide. Data were fitted to a two-site binding model by using custom written software, which resulted in two estimates for the equilibrium dissociation constants (K_{D1} and K_{D2}) (45).

Labeling of Antibodies. Antibodies were labeled by using Iodogen or Alexa 555/Alexa 647 carboxylic acid, succimidyl ester as described in refs. 27 and 47. For use in placental assays, antibodies were biotinylated in 0.1 M carbonate buffer (pH 8.5) by using 9 μg of EZ-link Sulfo-NHS biotin (Pierce, Rockford, IL) per milligram of antibody. Before use in studies, all labeled antibodies were compared with their unlabeled counterparts by using surface plasmon resonance to ensure that labeling had not altered their binding characteristics.

Pharmacokinetic Studies. Swiss–Webster mice were fed 0.1% Lugol (Sigma-Aldrich, St. Louis, MO) for 72 h before i.v. injection in the tail vein with either ^{125}I-labeled wild-type or mutated IgG1 (8–10 μg per mouse; five mice per group). Mice were analyzed by whole-body counting by using an AtomLab 100 counter (Shirley, NY) at the indicated times up to 168 h. To determine half-lives of the IgGs, data were fitted to a decaying biexponential model by using custom written software in MatLab (Mathworks, Natick, MA).

Analysis of Effects of the HN Mutant on IgG Clearance. Swiss–Webster mice were injected i.p. with ^{125}I-labeled human IgG1, followed by i.v. delivery of 500 μg of unlabeled wild-type human IgG1 or HN mutant 72 h later as described in ref. 31. Five mice per group were used. Persistence of radiolabeled human IgG1 was analyzed by whole-body counting with an AtomLab 100 counter at the indicated times. Statistical analyses were carried out by using Student's t test for a two-tailed distribution with unequal sample variance, and values of $P < 0.05$ were considered to be significantly different.

Analyses of Antibody Recycling. Endothelial cells (human microvascular endothelial cell 1; a generous gift of Francisco Candal, Center for Disease Control, Atlanta, GA) were transiently transfected by using Nucleofector technology (Amaxa, Cologne, Germany) with expression plasmids for human FcRn-GFP plus human β2-microglobulin or mouse FcRn-GFP plus mouse β2-microglobulin as described in refs. 27 and 31. Transfected cells were grown overnight in 24-well plates in phenol red-free Hams-12K medium. Eighteen to 22 hours after transfection, cells were pulsed with 250 μg/ml Alexa 647-labeled wild-type human IgG1 or 25 μg/ml Alexa 647-labeled HN mutant for 45 min at 37°C in a 5% CO_2 incubator. Cells were washed and chased in prewarmed (37°C) medium for 15 or 30 min and then washed and removed from the wells by trypsinization. In addition, for the 0-min chase, cells were washed with ice-cold PBS plus 0.02% sodium azide before trypsinization. Cells were analyzed by using a FACSCalibur flow cytometer (BD Biosciences, Franklin Lakes, NJ). Data were analyzed by using WinMDI 2.8 software (J. Trotter, The Scripps Research Institute, La Jolla, CA).

For fluorescence microscopy, cells were treated as above except they were seeded on coverslips immediately after transfection, and 18–22 h later, were pulsed with 20 μg/ml Alexa

555-labeled IgG. After pulsing, IgG-treated cells were washed, fixed with 3.4% paraformaldehyde, and mounted in Prolong (Invitrogen/Molecular Probes, Carlsbad, CA) for imaging.

Fluorescence Microscopy. Images of fixed cells were acquired with an Axiovert 200M inverted epifluorescent microscope by using a 1.4 N.A., ×100 PlanApo objective (Zeiss, Thornwood, NJ). Filter sets for GFP (lot no. C-11209; exciter HQ470/40X, dichroic Q495LP, emitter HQ525/50) and Alexa-555 (lot no. C-41201; exciter HQ545/30X, dichroic Q570LP, emitter HQ620/60m) were obtained from Chroma Technology (Brattleboro, VT). A 12-bit cooled CCD camera Orca 100, (Hamamatsu, Bridgewater, NJ) with a pixel size of 6.7 μm × 6.7 μm was used for image acquisition. All image data were acquired, overlaid, and processed by using custom written software in the programming language Matlab (Mathworks). Further details of microscopy methods are provided in the *Supporting Materials*, which is published as supporting information on the PNAS web site.

Placental Transfer Assay. Essentially the same methods as those described in ref. 30 were used. These studies are categorized as exempt by the Institutional Review Board for human studies at the University of Texas Southwestern Medical Center. Three milligrams of each of wild-type IgG1 or HN mutant (labeled with either biotin or ^{125}I) were added to the maternal compartment of the *ex vivo* placental model and transport to the fetal compartment analyzed by sample collection at the indicated times. After collection, samples were centrifuged at 1,500 × *g* for 10 min, and pellets were discarded. The amounts of IgG in the supernatant were determined by ELISA (for biotinylated IgG) or by γ-counting after precipitation with 10% TCA. ELISAs to detect biotinylated IgG were carried out as described in ref. 30. For use in ELISAs, neutravidin and HRP-goat anti human IgG (γ-chain specific) were purchased from Pierce and Sigma (St. Louis, MO), respectively. Transfer rates per hour were calculated between 30 or 60 min and 240 min after the start of each experiment, as follows:

$$\frac{\%\ \text{transfer (time } x) \ -\ \%\ \text{transfer (time } y)}{x - y\ \text{(in hours)}}. \qquad [1]$$

We thank Jinchun Zhou for assistance with the placental transport assays; Fernando Mateos for expert technical help; and Sripad Ram, Zhuo Gan, and Prashant Prabhat for help with the data analyses and figures. This study was supported by National Institutes of Health Grants R01 AI39167 and R01 AI55556.

1. Ghetie V, Popov S, Borvak J, Radu C, Matesoi D, Medesan C, Ober RJ, Ward ES (1997) *Nat Biotechnol* 15:637–640.
2. Shields RL, Namenuk AK, Hong K, Meng YG, Rae J, Briggs J, Xie D, Lai J, Stadlen A, Li B, *et al.* (2001) *J Biol Chem* 276:6591–6604.
3. Dall'Acqua W, Woods RM, Ward ES, Palaszynski SR, Patel NK, Brewah YA, Wu H, Kiener PA, Langermann S (2002) *J Immunol* 169:5171–5180.
4. Hinton PR, Johlfs MG, Xiong JM, Hanestad K, Ong KC, Bullock C, Keller S, Tang MT, Tso JY, Vasquez M, *et al.* (2004) *J Biol Chem* 279:6213–6216.
5. Lazar GA, Dang W, Karki S, Vafa O, Peng JS, Hyun L, Chan C, Chung HS, Eivazi A, Yoder SC, *et al.* (2006) *Proc Natl Acad Sci USA* 103:4005–4010.
6. Carter PJ (2006) *Nat Rev Immunol* 6:343–357.
7. Borvak J, Richardson J, Medesan C, Antohe F, Radu C, Simionescu M, Ghetie V, Ward ES (1998) *Int Immunol* 10:1289–1298.
8. Israel EJ, Taylor S, Wu Z, Mizoguchi E, Blumberg RS, Bhan A, Simister NE (1997) *Immunology* 92:69–74.
9. Dickinson BL, Badizadegan K, Wu Z, Ahouse JC, Zhu X, Simister NE, Blumberg RS, Lencer WI (1999) *J Clin Invest* 104:903–911.
10. Zhu X, Meng G, Dickinson BL, Li X, Mizoguchi E, Miao L, Wang Y, Robert C, Wu B, Smith PD, *et al.* (2001) *J Immunol* 166:3266–3276.
11. Haymann JP, Levraud JP, Bouet S, Kappes V, Hagege J, Nguyen G, Xu Y, Rondeau E, Sraer JD (2000) *J Am Soc Nephrol* 11:632–639.
12. Antohe F, Radulescu L, Gafencu A, Ghetie V, Simionescu M (2001) *Hum Immunol* 62:93–105.
13. Spiekermann GM, Finn PW, Ward ES, Dumont J, Dickinson BL, Blumberg RS, Lencer WI (2002) *J Exp Med* 196:303–310.
14. Kim JK, Tsen MF, Ghetie V, Ward ES (1994) *Eur J Immunol* 24:2429–2434.
15. Raghavan M, Bonagura VR, Morrison SL, Bjorkman PJ (1995) *Biochemistry* 34:14649–14657.
16. Martin WL, West APJ, Gan L, Bjorkman PJ (2001) *Mol Cell* 7:867–877.
17. Hinton PR, Xiong JM, Johlfs MG, Tang MT, Keller S, Tsurushita N (2006) *J Immunol* 176:346–356.
18. Ahouse JJ, Hagerman CL, Mittal P, Gilbert DJ, Copeland NG, Jenkins NA, Simister NE (1993) *J Immunol* 151:6076–6088.
19. Story CM, Mikulska JE, Simister NE (1994) *J Exp Med* 180:2377–2381.
20. Ober RJ, Radu CG, Ghetie V, Ward ES (2001) *Int Immunol* 13:1551–1559.
21. Zhou J, Johnson JE, Ghetie V, Ober RJ, Ward ES (2003) *J Mol Biol* 332:901–913.
22. Rodewald R (1976) *J Cell Biol* 71:666–669.
23. Wallace KH, Rees AR (1980) *Biochem J* 188:9–16.
24. Popov S, Hubbard JG, Kim J, Ober B, Ghetie V, Ward ES (1996) *Mol Immunol* 33:521–530.
25. Ghetie V, Ward ES (2000) *Annu Rev Immunol* 18:739–766.
26. Rojas R, Apodaca G (2002) *Nat. Rev Mol Cell Biol* 3:944–955.
27. Ober RJ, Martinez C, Vaccaro C, Zhou J, Ward ES (2004) *J Immunol* 172:2021–2029.
28. Ober RJ, Martinez C, Lai X, Zhou J, Ward ES (2004) *Proc Natl Acad Sci USA* 101:11076–11081.
29. Medesan C, Matesoi D, Radu C, Ghetie V, Ward ES (1997) *J Immunol* 158:2211–2217.
30. Firan M, Bawdon R, Radu C, Ober RJ, Eaken D, Antohe F, Ghetie V, Ward ES (2001) *Int Immunol* 13:993–1002.
31. Vaccaro C, Zhou J, Ober RJ, Ward ES (2005) *Nat Biotechnol* 23:1283–1288.
32. Kim JK, Firan M, Radu CG, Kim CH, Ghetie V, Ward ES (1999) *Eur J Immunol* 29:2819–2825.
33. Kabat EA, Wu TT, Perry HM, Gottesman KS, Foeller C (1991) *Sequences of Proteins of Immunological Interest* (US Dept of Health and Human Services, Bethesda, MD).
34. Claypool SM, Dickinson BL, Yoshida M, Lencer WI, Blumberg RS (2002) *J Biol Chem* 277:28038–28050.
35. Praetor A, Hunziker W (2002) *J Cell Sci* 115:2389–2397.
36. Ward ES, Zhou J, Ghetie V, Ober RJ (2003) *Int Immunol* 15:187–195.
37. Ghetie V, Hubbard JG, Kim JK, Tsen MF, Lee Y, Ward ES (1996) *Eur J Immunol* 26:690–696.
38. Junghans RP, Anderson CL (1996) *Proc Natl Acad Sci USA* 93:5512–5516.
39. Israel EJ, Wilsker DF, Hayes KC, Schoenfeld D, Simister NE (1996) *Immunology* 89:573–578.
40. Roopenian DC, Christianson GJ, Sproule TJ, Brown AC, Akilesh S, Jung N, Petkova S, Avanessian L, Choi EY, Shaffer DJ, *et al.* (2003) *J Immunol* 170:3528–3533.
41. Baker M (2005) *Nat Biotechnol* 23:1065–1072.
42. Weiner LM, Carter P (2005) *Nat Biotechnol* 23:556–557.
43. Wright A, Morrison SL (1997) *Trends Biotechnol* 15:26–32.
44. Foote J, Winter G (1992) *J Mol Biol* 224:487–499.
45. Zhou J, Mateos F, Ober RJ, Ward ES (2005) *J Mol Biol* 345:1071–1081.
46. Ober RJ, Ward ES (2002) *Anal Biochem* 306:228–236.
47. Kim JK, Tsen MF, Ghetie V, Ward ES (1994) *Eur J Immunol* 24:542–548.
48. Deisenhofer J (1981) *Biochemistry* 20:2361–2370.